www.czasopisma.pan.pl PAN www.journals.pan.pl
PAN
ARCHIVES OF ACOUSTICS
Vol. **41**, No. 4, pp. 747–755 (2016)

DOI: 10.1515/aoa-2016-0072

Numerical Analysis of Sensitivity of SAW Structure to the Effect of Toxic Gases

Tomasz HEJCZYK[(1)], Tadeusz PUSTELNY[(2)], Bartłomiej WSZOŁEK[(1)], Wiesław JAKUBIK[(3)], Erwin MACIAK[(2)]

[(1)] *ENTE Sp. z o.o.*
Gaudiego 7, 44-100 Gliwice, Poland; e-mail: t.hejczyk@ente.com.pl

[(2)] *Department of Optoelectronics, Silesian University of Technology*
Akademicka 2A, 44-100 Gliwice, Poland; e-mail: tpustelny@polsl.pl

[(3)] *Institute of Physics, Silesian University of Technology*
B. Krzywoustego 22b, 44-100 Gliwice, Poland; e-mail:wieslaw.jakubik@polsl.pl

(*received April 12, 2016; accepted September 18, 2016*)

The paper presents the results of numerical analysis of the SAW gas sensor in the steady and non-steady states. The effect of SAW velocity changes vs surface electrical conductivity of the sensing layer is predicted. The conductivity of the porous sensing layer above the piezoelectric waveguide depends on the profile of the diffused gas molecule concentration inside the layer. The Knudsen's model of gas diffusion was used.

Numerical results for the effect of gas CH_4 on layers: WO_3, TiO_2, NiO, SnO_2 in the steady state and CH_4 in the non-steady state in recovery step in the WO_3 sensing layer have been shown. The main aim of the investigation was to study thin film interaction with target gases in the SAW sensor configuration based on simple reaction-diffusion equation.

The results of the numerical analysis allow to select the sensor design conditions, including the morphology of the sensor layer, its thickness, operating temperature, and layer type. The numerical results basing on the code elaborated numerical system (written in Python language), were analysed. The theoretical results were verified and confirmed experimentally.

Keywords: surface acoustics wave SAW; Ingebrigtsen's formula; gas diffusion equations; gaseous acoustic sensors; numerical analyses of SAW structures.

1. Introduction

The main aim of the investigation was study thin film interaction with target gases in the SAW sensor based on simple reaction-diffusion equation (Matsumaga *et al.*, 2001; 2003). Diffusion equations provide theoretical bases for the analysis of physical phenomena like heat transport or mass transport in porous substrate. The paper summarises the acousto-electric theory, i.e. Ingebrigtsen's formula, dynamics gas diffusion concentration profiles, and predicts in recovery steps the influence of a thin semiconductor sensor layer with Knudsen's gas diffusion model on the SAW wave velocity in a piezoelectric acoustic waveguide (Hejczyk *et al.*, 2010).

Target gas molecules, like i.e. methane (CH_4), diffuse in the porous sensing layers from its outer plate to inside. By using a thin film semiconductor layer: WO_3 ($E_g = 2.7$ eV), TiO_2 ($E_g = 3.0$ eV), NiO ($E_g = 3.8$ eV), SnO_2 ($E_g = 3.7$ eV) (Porter, Hilal, 2004) we have succeeded in disclosing target gas methane concentration profiles inside the thin film under steady-state as well as them influence on the response of the SAW gas sensor (Hejczyk *et al.*, 2015; Kawalec *et al.*, 2008; Jasek *et al.*, 2011; 2012; Pustelny, Pustelny, 2009; Kawalec, Pasternak, 2008). Diffusion of gas molecules into the sensor layer will change its physical properties, especially the electrical conductivity. This effect causes a change in boundary conditions for wave propagation. Attenuation of the SAW changed also velocity of its propagation. In SAW sensors two types of effects may occur: electrical (acoustoelectrical) and mass ones. In this paper we considered only the electrical effect, important in a SAW sensor with a conducting sensor layer. The behavior of the gas concentration profile methane under non-steady-state conditions during recovery steps has been analysed. The paper presents the final equation describing time-dependent concentration profiles in the recovery step method.

Changes in the electrical properties of sensor layers depend on the concentration of gas molecules in the volume and also on the thickness, temperature, size of the gas molecules, layer morphology, and porosity of the sensing layer. A numerical analysis with using elaborated numerical program (in the Python system) of the impact of these parameters on a sensor response has been conducted. The obtained results are important for a proper construction of the SAW sensor. This analysis can be performed basing on the developed analytical model of a SAW sensor and supported gas diffusion dynamics equations for thin film semiconductor (Urbanczyk, Hejczyk, 2011; Hejczyk *et al.*, 2012).

2. Model of the SAWs gas sensor and influence of the diffusion gas on the acoustoelectric effect

The diffusion of gas particles into the sensor layer causes the formation of a certain profile of the distribution of concentration of these particles deep into the layer. The phenomenon of the diffusion of gas into the sensor layer is of essential importance in the case of a porous layer with a developed surface. Such layers are built up in expressly performed technological processes. A high porosity ensures a high sensitivity to the impact of gas (Urbanczyk, Hejczyk, 2011).

In order to optimise the structure of the sensor it is important to get an analytical model of the SAW sensor. A stationary model (in the steady state) was supported by time dependences permitting research of dynamic characteristics of the SAW gas sensor (Urbanczyk, 2011a).

In a sensor with an acoustic surface wave (SAW) the chemically active sensor layer is deposited on a piezoelectric waveguide (Fig. 1). In SAW sensors ambient gas on the electric conductivity (acoustoelectric phenomenon) of the sensor layer is influenced. This process becomes essential when the layer is porous. The Knudsen's diffusion (Urbanczyk, 2011b) is of a particular importance. The diameter of the pores is in the range from 1 or 2 to 100 nm. The Knudsen type diffusion is most essential in application of sensors. The profiles of the concentration depend on the gas molecules in the sensor layer, on values of the ratio of the constant reaction rate k_D, and diffusion coefficient D_K. The diffusion is a kinetic phenomenon and depends on time. The profile of the distribution of gas molecules in the layer changes depending on the flow of time as well as on response and recovery steps. Analysis of this phenomenon in time permits testing the regeneration stage of the sensor as a function of time.

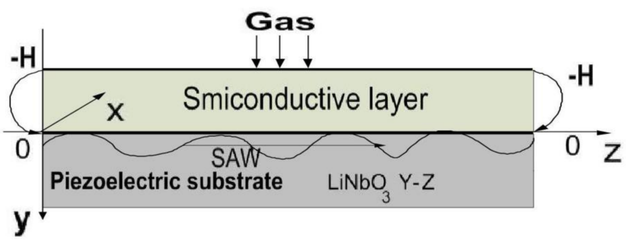

Fig. 1. Model of the analysed sensor structure.

The distribution of the concentration of gas molecules in the layer is the function of time t and the depth y in this resistance layer. The method manner of use of Fourier transformation by N. Matsunagi, G. Sakai, K. Shimanoe, N. Yamazone (Matsumaga *et al.*, 2003) has been presented. The concentration $C(y,t)$ in the recovery step can be expressed by Eqs. (1) and (2) (Matsumaga *et al.*, 2001):

$$C_A(y,t) = 4\cdot C_{A,S}\left[\sum_{n=1}^{\infty}\frac{1-(-1)^n}{2}\left(K_n - k_D t\frac{\beta_n^2 K_n}{\beta_n^2 + k_D(1-\exp(-\beta_n^2 t))}\right)\right], \tag{1}$$

$$K_n = \frac{\beta_n^2\exp(-\beta_n^2 t)}{n\pi(\beta_n^2+k_D)}\sin\frac{n\pi(H-y)}{2H}, \tag{2}$$

where $\beta_n = n\pi\sqrt{D_K}/2H$, $C_{A,S}$ is the concentration on the top surface of the sensor layer, n is the number of iterations, H is the thickness of the semiconducting sensor layer.

A target gas is switched off suddenly (Fig. 2) when concentration at initial $C_A(y,0)$ and the boundary conditions are $C_A(0,t) = C_{A,S}$ and $C_A(2H,t) = 0$ (Matsumaga *et al.*, 2003).

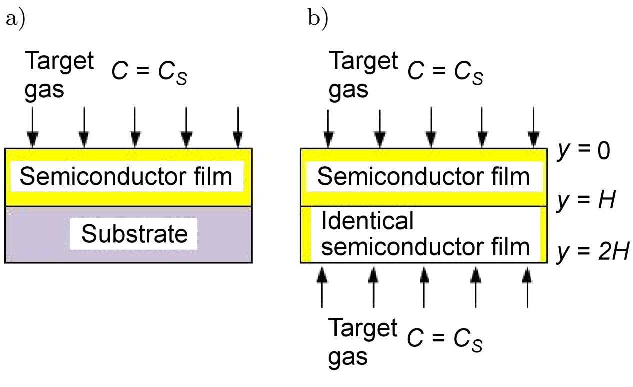

Fig. 2. Actual (a) and equivalent (b) models at the recovery step (Matsumaga *et al.*, 2003).

The formula presented above allows analysing changes in the concentration-time profile of the distribution of gas molecules.

Applying this solution in the analytical model of the SAW sensor (Eq. (3)) (Urbanczyk, 2011a;

Hejczyk, Urbanczyk, 2011), we can analyse the dynamics of the sensor response in the recovery state.

$$\begin{aligned}\frac{\Delta v}{v_0} &= -\mathrm{Re}\left\{\frac{\Delta k}{k_0}\right\}\\ &= -\frac{K^2}{2}\left[\sigma_{T_2}(1+aC_{A,y=0})\right.\\ &\quad\left.+\sum_{i=1}^{n-1}\sigma_{T_2}(y_i)f(y_i,\sigma_{T_2}(y_i))\right]^2 \Big/\\ &\quad\left\{\left[\sigma_{T_2}(1+aC_{A,y=0})+\sum_{i=1}^{n-1}\sigma_{T_2}(y_i)f(y_i,\sigma_{T_2}(y_i))\right]^2\right.\\ &\quad\left.+\left[1+\sum_{i=1}^{n-1}g(y_i,\sigma_{T_2}(y_i))\right]^2(v_0F_S)^2\right\}, \qquad (3)\end{aligned}$$

where: n is the number of sublayers and $F_S = \varepsilon_0 + \varepsilon_p^T$, $\sigma_{T_2} = \sigma_{T_1}\exp\left(\frac{E_g}{2k_B}\cdot\frac{T_2-T_1}{T_1T_2}\right)$, $T_1 = 300$ K, $\sigma_{T_1} = \sigma_0$, k_B is the Boltzman constant, E_g is the band gap energy, ε_0 and ε_p^T are, respectively, dielectric permittivity of the vacuum and piezoelectric substrate (upper subscript T means "in a constant stress condition"). In the expression (3) the functions f (4) and g (5) are the results of the transformation of the individual sublayer on the surface of a sensor waveguide (Fig. 1) and it has the form (Urbanczyk, 2011a; 2011b; Hejczyk, Urbanczyk, 2011).

$$f(y_i,\sigma(y_i)) = \frac{1-[\tanh(ky_i)]^2}{[1+\tanh(ky_i)]^2+\left[\tanh(ky_i)\dfrac{\sigma(y_i)}{\varepsilon_0 v_0}\right]^2}, \qquad (4)$$

$$g(y_i,\sigma(y_i)) = \frac{[1+\tanh(ky_i)]^2+\tanh(ky_i)\left[\dfrac{\sigma(y_i)}{\varepsilon_0 v_0}\right]^2}{[1+\tanh(ky_i)]^2+\left[\tanh(ky_i)\dfrac{\sigma(y_i)}{\varepsilon_0 v_0}\right]^2}, \qquad (5)$$

and $\sigma(y_i) = \sigma_0[1 + a\cdot C_A(y_i)]$, v_o is the SAW velocity, k is the acoustic wave number ($k = 2\pi/\lambda$).

The distribution of gas molecules in the sensor layer in time and space depends on such parameters as: reaction rate k_D, the constant of diffusion D_K, time, temperature, and other.

The accuracy of numerical calculations depends on the number of iterations n. It is easy to see that profiles of concentration depend strictly on the diffusion parameters. The results obtained at various constants diffusion D_K have been compared with the results obtained by Matsunaga and Sakai and others (Hejczyk, Urbanczyk, 2011). The results are convergent. The profile presented in Fig. 3 concerns gas in the case of a fixed number of iterations n = 10–100, a fixed time t = 0.1 ns, a constant reaction $k_D = 10^5$ s^{-1}, and values of the constants of Knudsen's diffusion $D_K = 10^{12}$ nm^{2}s^{-1}. The accuracy of the method increases with the number of iterations. The authors have also found, similarly to what is quoted in (Matsumaga, 2003), that the analysis in non-stationary states in recovery time is of essential importance within the range from $t = 10^{-14}$ sec to 10^{-3} (Figs. 3–6).

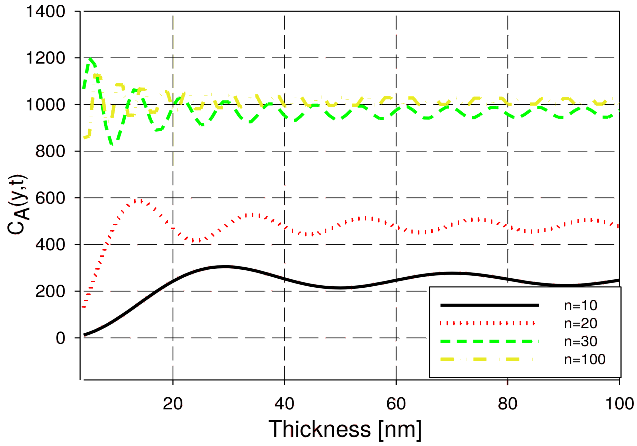

Fig. 3. Profiles of gas concentration depending on the number of iterations n = 10, 20, 30, 100, at Cs = 10000 ppm, t = 0.1 ns, $k_D = 10^5$ s^{-1}, $D_K = 10^{12}$ nm^{2}s^{-1}.

Calculations of the profile according to the Eqs. (1), (2) (in the Python software) have been made. The graphic user interface in Python allows to change all parameters in Eqs. (1), (2). The influence of the following parameters on the profile of the concentration of gas molecules in the layer was simulated: the reaction constant k, the coefficient of diffusion D_K, time t, and number of iterations n (Matsumaga *et al.*, 2001; Urbanczyk, 2011a). Exemplary results, illustrating the shape of the profile of concentration in the sensor layer at recovery step, are presented in Figs. 3–6.

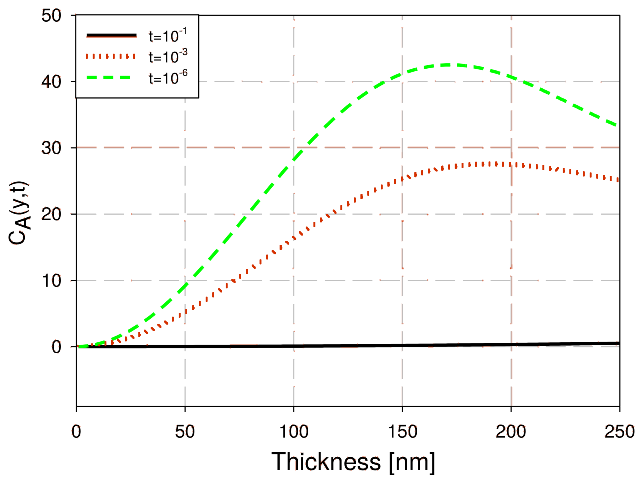

Fig. 4. Profiles of the concentration of gaseous molecules depending on the thickness of the layer in time $t = 10^{-6}$, 10^{-3}, 10^{-1} s, at Cs = 10000 ppm, n = 6, $k_D = 10^6$ s^{-1}, $D_K = 10^6$ nm^{2}s^{-1}.

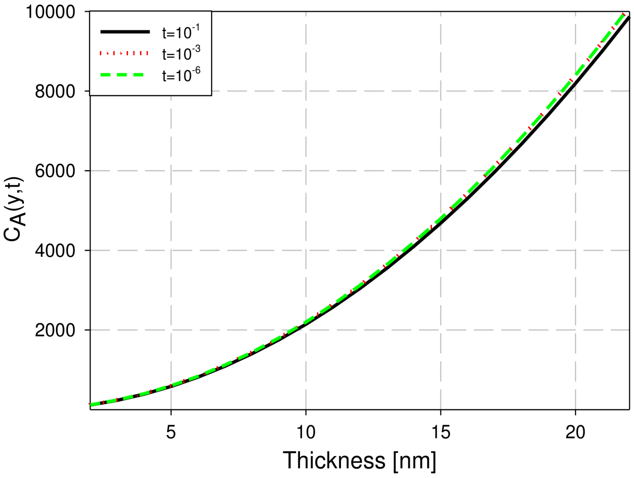

Fig. 5. Profiles of the concentration of gaseous molecules depending on the thickness of the layer in time $t = 10^{-6}$, 10^{-3}, 10^{-1} s, at $Cs = 10000$ ppm, $n = 1$, $k_D = 0\ \mathrm{s}^{-1}$, $D_K = 10^5\ \mathrm{nm}^2\mathrm{s}^{-1}$.

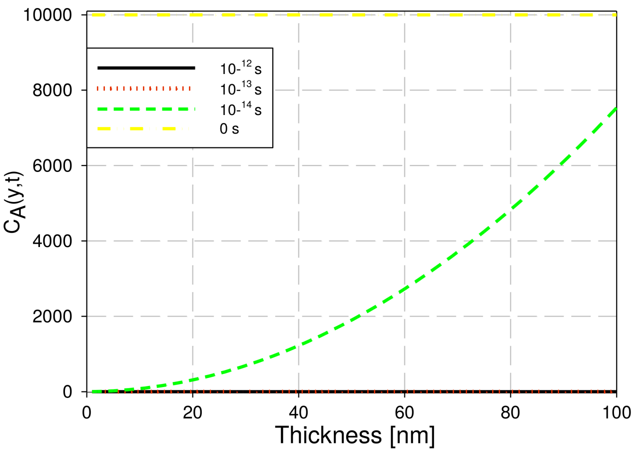

Fig. 6. Profiles of the concentration of gaseous molecules depending on the thickness of the layer in time $t = 10^{-14}$, 10^{-13}, 10^{-12} s, at $Cs = 10000$ ppm, $n = 50$, $k_D = 10^4\ \mathrm{s}^{-1}$, $D_K = 10^4\ \mathrm{nm}^2\mathrm{s}^{-1}$.

The main aim of the simulation was to comprehend the essence of the dynamic phenomena occurring in the SAW sensor layer in the absence of gas in the recovery step. It is possible to check the effect of the rate of the reaction from the gas molecules in the semiconductor layer and find an approximate time of the recovery processes until the concentration profile does not reach the zero state. The results of the analysis above indicate changes of concentration profiles of the diffusing gas in the sensor layer monotonically in time.

3. Numerical analysis in steady-state of the acoustoelectric interaction in the sensing layers WO_3, TiO_2, NiO, SnO_2

From the above characteristics results that the SAW sensor response depends on the concentration (Fig. 7a) – with the increase of concentration of gas

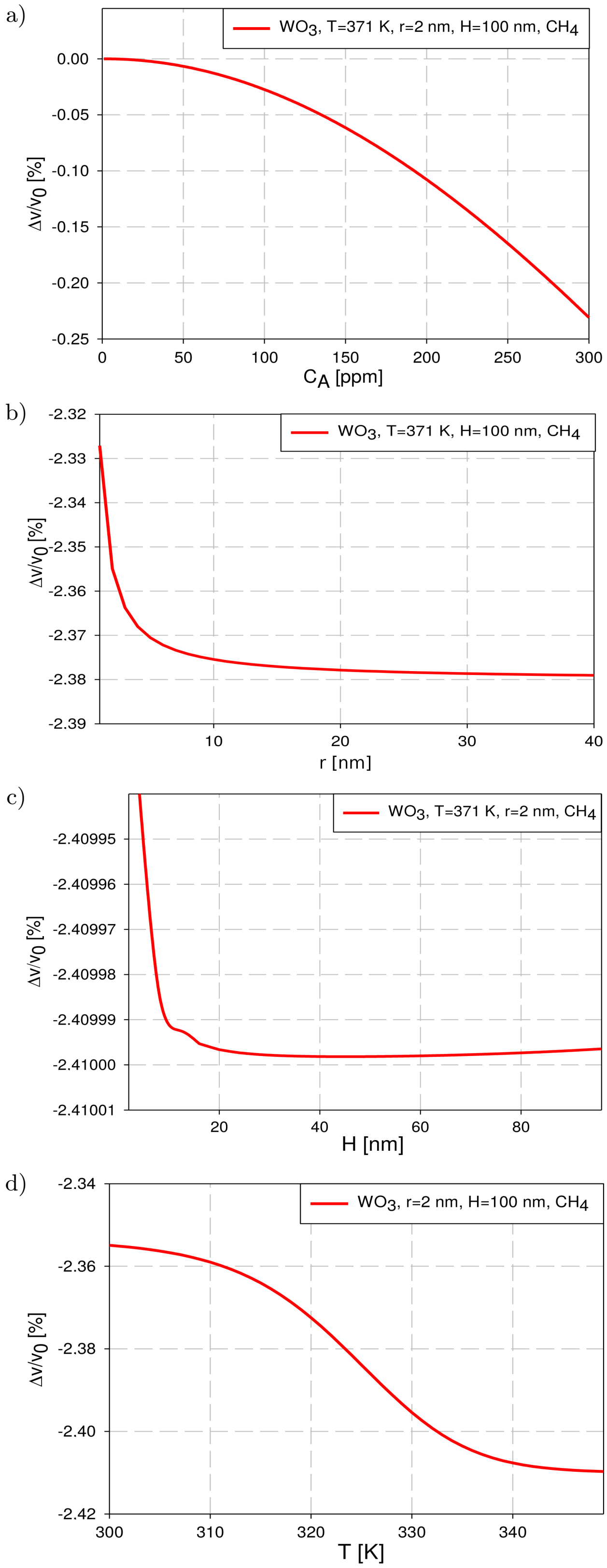

Fig. 7. SAW wave velocity changes vs: a) concentration of CH_4, b) pore radius, c) sensing layer thickness, and d) temperature. The results are presented assuming the following values have become involved: $\sigma_s = v_0 C_S = 4.7 \cdot 10^{-8}\ \Omega^{-1}$, sensitivity coefficient $a = 1\ \mathrm{ppm}^{-1}$, thickness of the sensor layer 100 nm, temperature 371 K, pore radius 2 nm, WO_3 layer ($E_g = 2.7$ eV).

the response of SAW sensor changed. In the case of interaction of methane on the WO_3 sensor layer the most significant changes in the response characteristics depending on the pore radius from 2 to 20 nm were observed (Fig. 7b). It should be noted that the assumed type Knudsen diffusion depends on the porosity, characterised by the pore radius. Interesting characteristics depending on thickness were obtained (Fig. 7c).

There are two areas. The first one with a very strong interaction depends on the layer thickness smaller than 30 nm. There are rapid changes in the response of sensor. When the thickness layer is so small the influence decreases completely. In the response depending on the thickness of the sensor is the second area of weaker interactions below the thickness of 60 nm. The response is slower. Between areas of strong and weak interaction the optimum thickness range from 30 nm to 60 nm is observed. Maximum changes for the layer thickness approx. 50 nm occur. The response of the sensor depending on the temperature was presented (Fig. 7d). The growth of the response depending on temperature is observed.

The results of the numerical analysis serve as the basis for the optimisation of the parameters of the sensor layer reaching maximum dynamics and sensitivity of the sensor. The acoustoelectric interaction of the SAW with electrical charge carriers distributed in the sensor layer was calculated in compliance with the profile resulting from diffusion of the gas molecules in the ambient atmosphere. Acoustoelectric interaction of surface waves with charge carriers in the layer of the sensor are formed by the diffusion of the methane (hydrocarbon molecules) CH_4. Interactions in the steady and non-steady state in recovery step were analysed numerically in Python. Sensor responses (relative changes in wave propagation velocity with respect to the parameter energy gap – E_g) for layers: WO_3 ($E_g = 2.7$ eV), TiO_2 ($E_g = 3.0$ eV), NiO ($E_g = 3.8$ eV), SnO_2 ($E_g = 3.7$ eV) are shown in Fig. 8. The following diagram shows the results of the analysis of the sensor response vs temperature depending on the type of layer in the steady state.

The optimal operating temperature of the sensor is slightly higher than 340 K (Hejczyk *et al.*, 2012).

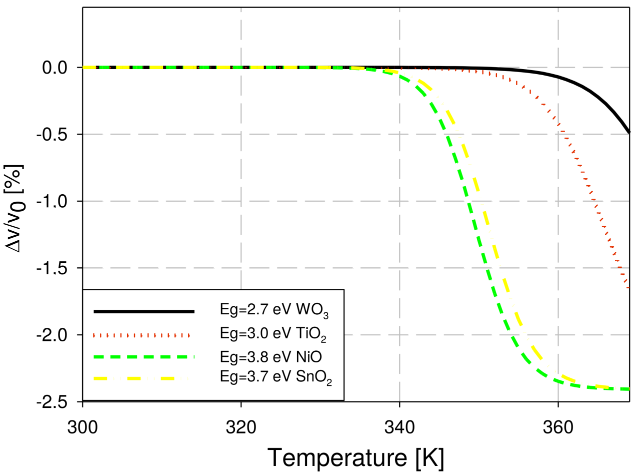

Fig. 8. SAW wave velocity changes vs temperature of the sensor layer of WO_3 layer ($E_g = 2.7$ eV), TiO_2 ($E_g = 3.0$ eV), NiO ($E_g = 3.8$ eV), SnO_2 ($E_g = 3.7$ eV), $H = 50$ nm, concentration 300 ppm, pore radius 2 nm, methane M = 16 g/mol.

4. Numerical analysis of the acoustoelectric interaction in the sensing layer in the recovery step

This problem was analysed numerically, assuming a constant concentration of the gas molecules at the surface of the sensor layer and in its surroundings. Changes of the relative velocity of the wave were determined numerically, viz. the concentration of the gas molecules on the surface $C_{A,S}$, the values of the mean radius of the pores r, and the thickness of the layer H and temperature T.

The analysis in the non-steady state was performed. Time in range from $t = 10^{-9}$ to $t = 10^{-1}$ sec was changed. The task was prepared basing on the assumption that after the time $t = 10^{-1}$ sec the profile of the concentration of the gas molecules in the sensor layer reach its steady state.

The analysis of the recovery state, shown in Figs. 9–12, allows to observe temporal changes in the response of the sensor. The response of the WO_3 semiconductor layer with an energy gap $E_g = 2.7$ eV on the methane (CH_4) in the recovery state depending on the gas concentration (Fig. 9), the dimensions of the radius of the pores (Fig. 10), the layer thickness (Fig. 11), and temperature (Fig. 12) were analysed.

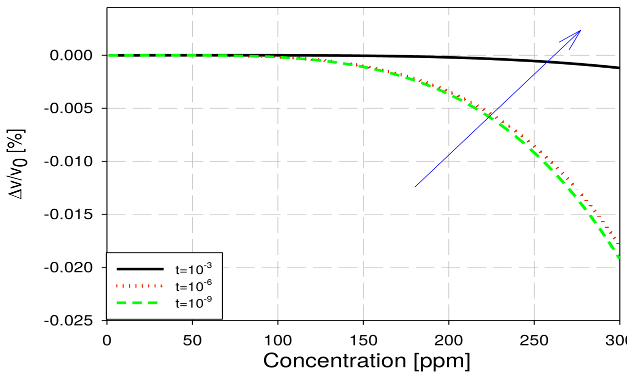

Fig. 9. SAW wave velocity changes in the recovery state vs gas concentration of CH_4 at layer thickness 50 nm, pore radius 2 nm, concentration 300 ppm, temperature 300 K at times $t = 10^{-9}$, 10^{-6} to 10^{-3} sec for $k_D = 10^4$ s^{-1}, $D_K = 10^{12}$ nm^{2}s^{-1}, $n = 4$, WO_3 layer ($E_g = 2.7$ eV), methane M = 16 g/mol.

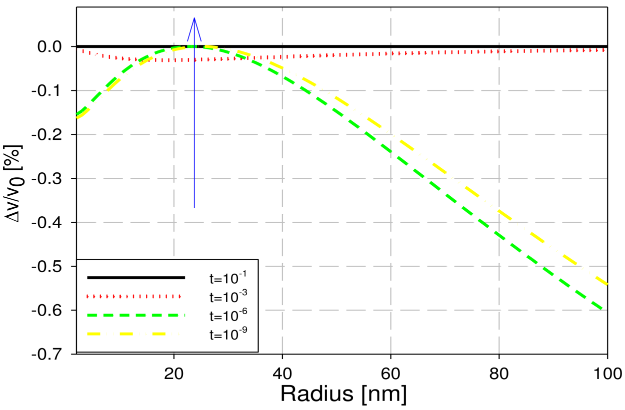

Fig. 10. SAW wave velocity changes in the recovery state vs radius of CH_4 at layer thickness 50 nm, concentration 300 ppm, temperature 305 K at times $t = 10^{-9}$, 10^{-6}, 10^{-3} to 10^{-1} sec for $k_D = 10^4$ s^{-1}, $D_K = 10^{12}$ nm^{2}s^{-1}, $n = 4$, WO_3 layer ($E_g = 2.7$ eV), methane M = 16 g/mol (CH_4).

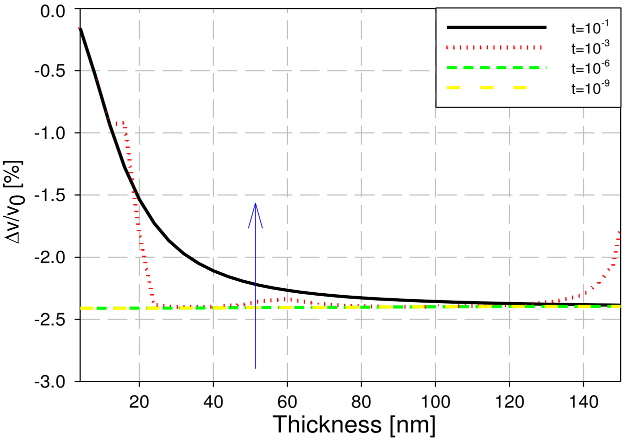

Fig. 11. SAW wave velocity changes in the recovery state vs thickness at pore radius layer 2 nm, concentration 300 ppm, temperature 300 K at times $t = 10^{-9}$, 10^{-6}, 10^{-3} to 10^{-1} sec for $k_D = 10^4$ s^{-1}, $D_K = 10^{12}$ nm^{2}s^{-1}, $n = 4$, WO_3 layer ($E_g = 2.7$ eV), methane M = 16 g/mol (CH_4).

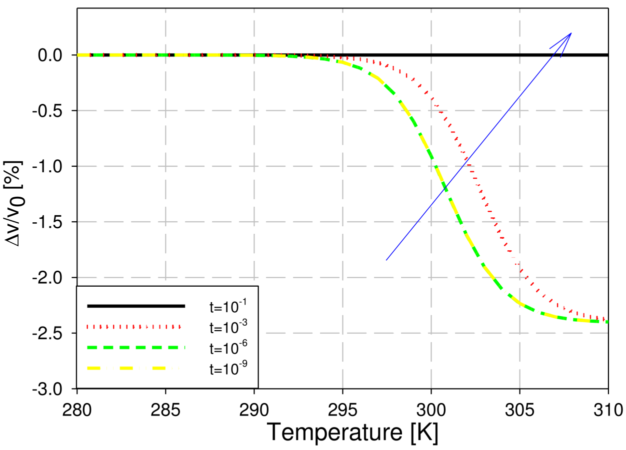

Fig. 12. SAW wave velocity changes in the recovery state vs temperature at pore radius layer 2 nm, thickness layer 50 nm, concentration 300 ppm at times $t = 10^{-9}$, 10^{-6}, 10^{-3} to 10^{-1} sec for $k_D = 10^4$ s^{-1}, $D_K = 10^{12}$ nm^{2}s^{-1}, $n = 4$, WO_3 layer ($E_g = 2.7$ eV), methane M = 16 g/mol (CH_4).

The analysis of numerical profiles in the response were made. Formula responsible for the concentration profile in the response state is shown below. In the response state, for a short response the time profile varies with time in accordance with the following formula:

$$C_A(y_i,t) = C_{A,S}\left[1 - \frac{2}{\pi}\sum_{n=1}^{\infty}\frac{1-(-1)^n}{n}\left[\exp(-\beta_n^2 t) + \frac{k_D\left(1-(1+\beta_n^2 t)\exp(-\beta_n^2 t)\right)}{\phi_n^2 + k_D(1-\exp(-\beta_n^2 t))}\right] \cdot \sin\frac{n\pi(H-y_i)}{2H}\right], \tag{6}$$

where:

$$\beta_n = \frac{n\pi\sqrt{D_K}}{2H},$$

$C_{A,S}$ is the concentration on the top surface of the sensor layer ($y = -H$), H is the thickness of the semiconducting sensor layer, n is the number of iterations.

It should be noted, by analogy to charging and discharging the capacitor processes, that adsorption and desorption demonstrate similarity to these processes. The charge in the charging process is stored – it reaches a predetermined value. During unloading the charge reaches the zero value – the case of electronic short circuit to ground. The following collective characteristics of the sensor in the response state in Fig. 13 are presented.

As compared to the recovery stage characteristics, it is easy to see, the response processes have a completely opposite nature of change. In the case of adsorption (sensor response) the characteristics tend to a value determined by the relative change of velocity depending on parameters such as concentration, porosity, thickness, and temperature of the sensor layer. In the case of desorption (regeneration) characteristics tend to zero. It is consistent with the expectations because processes by boundary conditions and initial conditions were determined.

Below three-dimensional characteristics of response and regeneration of the SAW sensor response were shown.

Regeneration occurs after a period of several milliseconds Figs. 9–12. From the analysis of the graphs presented above for the response and response processes in Fig. 13 it results that the the concentration profile is established after a period of several microseconds. These processes in Fig. 14 are illustrated. Dynamic responses of the SAW sensor in the state response and recovery were presented.

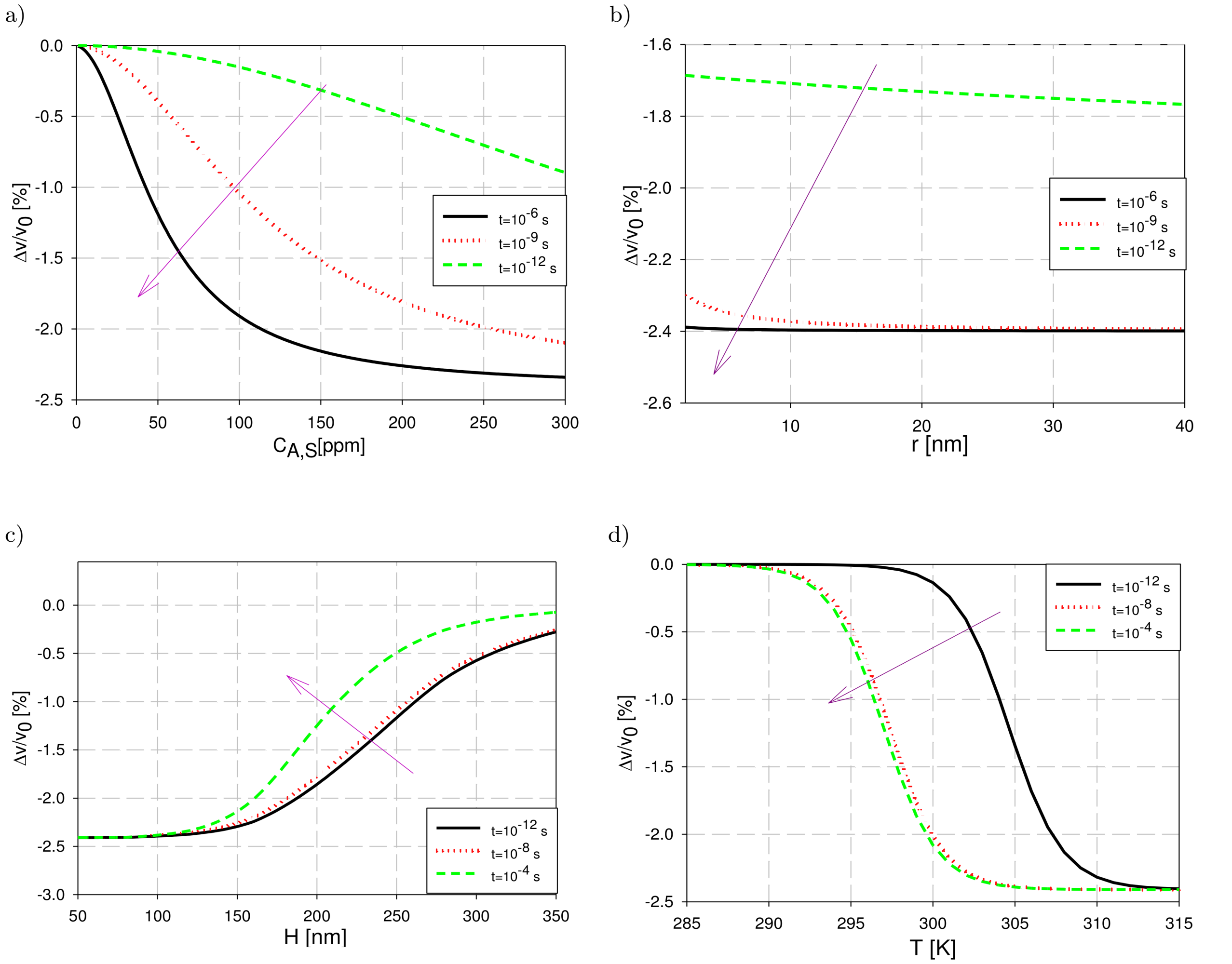

Fig. 13. SAW wave velocity changes in transient state (response) vs: a) gas concentration of CH_4, b) layer thickness, c) pore radius and d) temperature at times $t = 10^{-12}$ to 10^{-3} sec for $k_D = 10^{12}$ s^{-1}, $D = 10^{12}$ nm^2s^{-1}, WO_3 layer ($E_g = 2.7$ eV) (Hejczyk *et al.*, 2011).

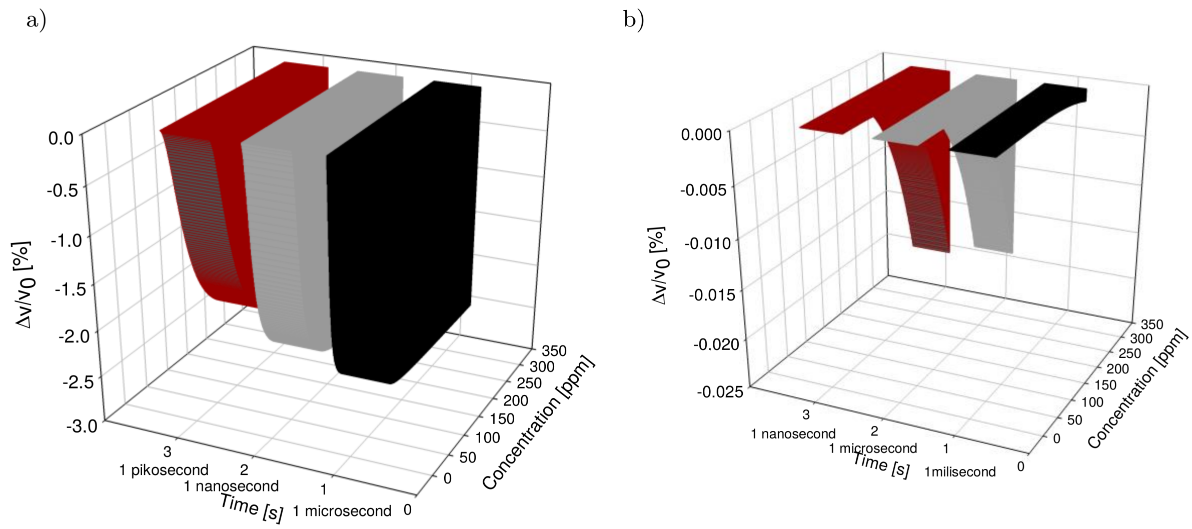

Fig. 14. Collective representation of time characteristics for methane in the state (the response of the sensor depending on the concentration of gas: a) response (concentration rising during adsorption), b) regeneration (during desorption after cutting off the gas supply).

5. Experimental results

Nature of the response of the sensor depends on the processes of adsorption, diffusion, and desorption. Temperature and concentration of gas molecules and the properties of the sensor layer: the thickness, porosity has influence on the character of these processes. In practice, the measurement is normalised. It is possible to compare the response of sensors. From the time characteristics of the response of the sensor conclusions can be meade about the properties of the layer sensor and the assumed parameters of the sensor layer can be verified. The response characteristics are determined experimentally. The analysis shows that the processes in the sensor layers are instantly performed in microseconds. The results obtained from the theoretical analysis should be considered in studying the dynamics response of the sensor and its verification. Time characteristics taking into account the inertia of the measuring chamber in Fig. 15 is shown.

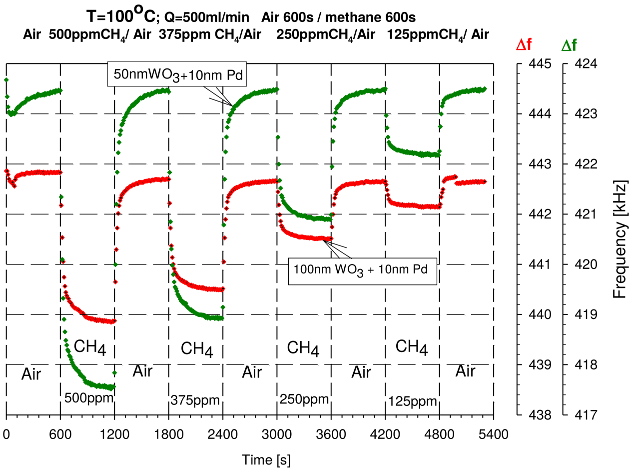

Fig. 15. Response of SAW sensor Δf with a WO_3 + Pd layer on methane, 50 and 100 nm thickness for concentration from 125 to 500 ppm in air. Temperature of the sensor 100°C.

The response and regeneration processes depend on the time when a fixed composition of gas mixture in the measuring chamber is reached, approx. 1–5 seconds.

6. Summary

Basing on the mechanism of Knudsen's diffusion of gas molecules in a porous sensor layer, the profiles of the concentration of gas molecules in a steady-state layer have been determined. The analysis of interaction on methane depending on type of sensor layer for methane (CH_4) and analysis in recovery step for methane (CH_4) are presented. The numerical calculations for a semiconductor layer of WO_3 ($E_g = 2.7$ eV) have been made.

Assuming the mechanism of occurring of type Knudsen diffusion of gas molecules in porous sensor layer, the profiles of the concentration of gas molecules in the sensor layer, dependent from time, have been determined. The profiles in the non-steady state in the recovery step basing on diffusion-reaction equations have been simulated and analysed.

Relative changes in the velocity of the surface wave as the result of the acoustoelectric effect depending on numerous parameters of the sensor and its environment have been determined. The results of the numerical analysis from parameters: concentration of gas molecules in the environment, the thickness and porosity of the sensor layer, and the temperature of the sensor on changes of the velocity of the propagation of Rayleigh's wave have been presented.

The recovery state in the range of time from 10^{-9} to 10^{-3} sec is distinctly visible. The performed analyses indicate that the steady state of responses of the sensor is achieved after a few milliseconds, depending on the parameters of the sensor layer: k, D_K, E_g, T, thickness H, gas concentration $C_{A,S}$, and type of gas.

Usefulness of the theoretical and experimental studies of the analytical model for designing the parameters of a SAW sensor has been confirmed. The theoretical results were verified and confirmed experimentally for the selected layered sensing structures.

Acknowledgments

The work is partially financed by the NCBR within the grant No: UOD-DEM-1-243/001 and by the Polish National Science Centre "NCN" within the grant 2012/07/B/ST7/01 471.

References

1. Hejczyk T., Urbanczyk M. (2011), *WO_3-Pd Structure in SAW Sensor Hydrogen Detection*, Acta Physica Polonica A, **120**, 4, 616–620.
2. Hejczyk T., Urbanczyk M., Jakubik W. (2010), *Analytical Model of Semiconductor Sensor Layers in SAW Gas Sensors*, Acta Physica Polonica A, **118**, 6, 1148–1152.
3. Hejczyk T., Urbanczyk M., Pustelny T., Jakubik W. (2015), *Numerical and Experimental Analysis of the Response of a SAW Structure with WO_3 layers an Action of Carbon Monoxide*, Archives of Acoustics, **40**, 1, 19–24.
4. Hejczyk T., Urbanczyk M., Witula R., Maciak E. (2012), *SAW sensors for detection of hydrocarbons. Numerical analysis and experimental results*, Bulletin of the Polish Academy of Sciences: Technical Sciences, **60**, 3, 589–595.
5. Jasek K., Miluski W., Pasternak M. (2011), *New approach to saw gas sensors array response measurement*, Acta Physica Polonica A, **120**, 4, 639–641.
6. Jasek K., Neffe S., Pasternak M. (2012), *SAW sensor for mercury vapour detection*, Acta Physica Polonica A, **122**, 5, 825–828.

7. Kawalec A., Pasternak M. (2008), *Microwave humidity sensor based on surface acoustic wave resonator with nafion layer*, IEEE Transactions on Instrumentation and Measurement, **9**, 57, 2019–2023.

8. Kawalec A., Pasternak M., Jasek K. (2008), *Measurements results of SAW humidity sensor with nafion layer*, European Physical Journal: Special Topics, 154, 121–126.

9. Matsumaga N., Sakai G., Shimonoe K., Yamazoe N. (2001), *Diffusion equation-based study of thin film semiconductor gas sensor-response transient*, Sensors and Actuators B, **83**, 216–221.

10. Matsumaga N., Sakai G., Shimonoe K., Yamazoe N. (2003), *Formulation of gas diffusion dynamics for thin film semiconductor gas sensor based on simple reaction-diffusion equation*, Sensors and Actuators B, **96**, 226–233.

11. Porter J., Hilal H.S. (2004), *Thermodynamic correlations and band gap calculations in metal oxides*, Elsevier, Progress in Solid State Chemistry, **32**, 207–217.

12. Pustelny B., Pustelny T. (2009), *Transverse acoustoelectric effect applying in surface study of GaP: Te(111)*, Acta Physica Polonica A, **116**, 3, 383–384.

13. Urbanczyk M. (2011a), *Analytical model of a SAW gas sensor*, WIT Transactions on Computational Methods and Experimental Measurements, Proceedings of the CMEM11, WIT Press Southampton, **48**, 229–239.

14. Urbanczyk M. (2011b), *Gas Sensors on the base of Surface Acoustic Wave* [in Polish], Monograph, **213**, Edited by SUT, Gliwice.

15. Urbanczyk M., Hejczyk T. (2011), *Analysis of nonsteady state in SAW gas sensors with semiconducting sensor layers*, Acta Phys. Polonica A, **120**, 4, 789–793.